International Journal of Advanced Technology and Engineering Exploration, Vol 9(95)
ISSN (Print): 2394-5443 ISSN (Online): 2394-7454
http://dx.doi.org/10.19101/IJATEE.2021.876215

Research Article

Modelling of viscosity equation for liquid-phase HCFO-1233zd(E)

Donny Agvie Putratama and I Made Astina*
Faculty of Mechanical and Aerospace Engineering, Institut Teknologi Bandung, Bandung, Indonesia

Received: 19-June-2022; Revised: 20-October-2022; Accepted: 23-October-2022

Abstract
Refrigerant is one source of greenhouse gas emissions affecting global warming. New eco-friendly refrigerants are needed to replace old-generation refrigerants. Trans-1-Chloro-3,3,3-trifluoropropene (HCFO-1233zd(E)) is an attractive refrigerant due to its low global warming and ozone depletion potential. It's thermophysical properties play an essential role in analyzing thermal and process systems. The viscosity can be derived using experiments or by using calculations. This research developed and evaluated an extended-corresponding state (ECS) and excess-entropy scaling (EES) models. The development of both models refers to the available viscosity experimental data. Symbolic regression is used in developing the EES model, whereas weighted regression is for the ECS model. Both models were evaluated and compared to each other to reveal their accuracy by comparing the available experimental data. The average absolute deviation of the developed ECS and EES models are 1.59% and 1.86%, respectively. By assessing the extrapolation behavior, both models can predict the viscosity of HCFO-1233zd(E) in the liquid phase from the triple point up to a temperature of 500 K and a pressure of 50 MPa.

Keywords
HCFO refrigerants, HCFO-1233zd(E), Viscosity, Extended-corresponding state, Excess-entropy scaling.

1.Introduction
Ozone depletion and global warming, which are two environmental problems, arise due to human activities releasing emission gases that contain halon gases, refrigerants, carbon dioxide (CO_2), methane (CH_4), and nitrous oxide (N_2O) [1]. Global warming occurs due to increased contamination of greenhouse gases in the atmosphere. Although the greenhouse gases contribute to global warming, they may maintain the earth's temperature level so that it is warm enough to be habitable. Heat-trapping gases such as CO_2, chloro fluoro carbon (CFC), hydro fluoro carbon (HFC), hydro chloro fluoro carbon (HCFC), and CH_4 trap the sun's heat in the earth and thus leading to global warming. As CFC, HFC, and HCFC are groups of refrigerants, finding new environmentally friendly refrigerants, which have low global warming potential (GWP) and low ozone-depleting potential (ODP), can solve the global environmental problems.

The substitution of low GWP refrigerants such as hydro chloro fluoro olefin (HCFO) and hydro fluoro olefin (HFO) is considered as a suitable refrigerant due to their properties to develop thermal systems either work as refrigeration or heat pump and power generation [2].

Unfortunately, there are only a few experimental data available in the public literature on HCFO refrigerants. Since difficulties exists in direct measurements of transport properties under specified conditions for science and engineering interests, a predicted model is required to obtain viscosity values for these low GWP and ODP refrigerants. HFO refrigerants are one of the alternative refrigerants that may be used as a substitute for HFC-134a, which is still exists in air conditioning systems. Older refrigerants generally have higher GWP and ODP compared to newer refrigerants.

The cost of operating personnel, lab analyst, and using measurement tools may be expensive. On the other hand, many researchers have tried implementing artificial intelligence to predict viscosity with high accuracy while maintaining minimum operating costs. This study aims to provide

*Author for correspondence

prediction methods by applying machine learning and AI to viscosity models using the latest dataset of refrigerants.

Existing models for calculating refrigerants have been introduced by researchers in the last decade to increase the accuracy of predicting thermodynamic and thermophysical properties. In this study, two approaches are involved to estimate the viscosity of a fluid: experimental research and theoretical research. The theoretical approach refers to natural phenomena to create mathematical models in proving the theory, while the empirical approach verifies theoretical predictions using experiments or measurements. Up to now, few measurements regarding HFO and HCFO have been conducted to acquire thermophysical properties experimentally or theoretically. This research developed a new correlation for HCFO-1233zd(E) using a predictive method for upcoming refrigerant development regarding HCFOs.

Global warming has become a common environmental problem in the world. The increasing use of refrigeration and air conditioning in developing countries means that HFC emissions contribute about 1% of global greenhouse gas emissions but grow by 8–9% annually. Additionally, an amendment to the Montreal Protocol adopted in Kigali Protocol in October 2016 requires the weighted value reduction of GWP of working fluids used in thermal systems either as heat pumps or power generation [3]. To preserve the environment, refrigerants with high GWP and ODP must no longer be used in thermal systems under the Kigali protocol. In addition to these environmentally friendly requirements, technical criteria such as non-flammability, chemical stability in operation conditions, the short shelf life in the atmosphere, non-toxicity, positive pressure at lowest operation temperatures, and good thermodynamic performance in the application are most criteria for best future refrigerants. The analysis and design of the thermal system equipment require thermodynamic and transport properties. With the hope of being able to reduce the production of ozone-depleting substances and to contribute within the world of thermophysics, viscosity model development is essential to prepare fluid transport properties for HCFO-1233zd(E). This article is presented in several sections, starting with an introduction, and continuing with a literature review related to viscosity and art in its modelling, the methods, results, and discussions, and finally closed with conclusions.

2.Literature review

Substitute refrigerants is a heated debate around greenhouse gas issues. A few haloalkanes (HCFOs) have been proposed to address nature concerns and are accepted as substitutes for HFCs. HCFOs are unsaturated HFCs, and since their unsaturated characteristics are beneficial, their life expectancies are moderately shorter than conventional HFCs. Therefore, the GWPs of the HCFOs are exceptionally small. One of the substitute refrigerants analyzed in this study is HCFO-1233zd(E). This HCFO has the chemical formula $CF_3CH=CHCl$ and is often known as trans-1-chloro-3,3,3-trifluoropropene, which is a non-flammable [4], has a normal boiling point of 291.47 K [5], and is more friendly environment than HFC due to GWP (100 years) of 7, an atmospheric lifetime of 26 days, and ODP of 0.0005 [6]. This HCFO is also suitable for low-pressure centrifugal chillers offering better capacity and similar efficiency to HFO-1234, which is most often used to cool large buildings, so that it becomes a friendly refrigerant. Additionally, it may also be used for organic Rankine cycles.

Properties data relating to thermodynamics and transport of HCFO-1233zd(E) were reported by several researchers. Hulse et al. [7] reported the data for the critical constants, vapor pressures, saturated-liquid densities, ideal-gas heat capacities, and surface tensions. Newer data for vapor pressure and density in the gaseous phase were measured by Yin et al. [8]. One of the transport properties to be interested in this study is viscosity. These data are required to develop a thermodynamic equation of state (EOS). The EOS plays an important role in predicting thermodynamic properties and is commonly used to analyze and design thermal systems. The measurements of viscosity are the essential data required in analysis and design.

Less data of viscosity for HCFO-1233zd(E) are available due to this refrigerant is newer. Meng et al. [9] measured viscosity using a vibrating wire viscometer covering a temperature range from 243 K to 373 K and pressures up to 40 MPa. Based on the accurate experimental data, Meng et al. developed a viscosity correlation. In the same year, Alam [10] measured viscosity using tandem capillary tubes and developed viscosity correlation from his experimental data. Cui et al. [11] proposed a correlation at saturation state, which was given in a polynomial equation. Recent data for this refrigerant were reported by Zhao et al. [12]. These data cover in saturated liquid for viscosity, surface tension and

thermal diffusivity. Unfortunately, most of the data range does not cover the application range. The predictive data from a mathematical model is also useful if the model has high accuracy. Referring to scarcely available data, fluid-phase data become a focus of this study to develop extended corresponding state (ECS) and excess entropy scaling (EES) models.

Entropy values, which can be derived from the EOS, are required to develop the EES model. Recently available EOS for HCFO-1233zd(E) are developed by Mondejar et al. [5], Budiarso and Astina [13], and Akasaka and Lemmon [14].

Modelling fluid properties becomes a challenge when available data are limited. Even without data, it can be predictable. The corresponding state approach is becoming one of the most popular methods for this situation. However, data is still needed to validate. Teraishi et al. [15] proposed universal parameters applied to refrigerants with critical point and acentric factor as parameters to the ECS model. This correlation only focuses on saturation thermodynamic properties. Therefore, a lot of effort is still needed for the transport. Otherwise, the EES model proposed by Fouad and Vega [16] was applied to HFC and HFO. Residual entropy scaling theory coupled with a generalized chart parametrization method proposed by Li et al. [17]. They applied the method for HFC, HFO, CO_2, dan natural gas. Study and measurement of data on HCFO-1233zd(E) are still very rare because this fluid is still relatively new and proposed as a refrigerant.

3.Methods and formulation

3.1Mathematical modelling

Mathematical modelling is a creating process of representations of real-world scenarios into the mathematical formulation to make predictions or provide insights. The practice of mathematical models to interpret problems in engineering, science, stock trading, forex trading or other activities including transportation and military plays a huge role in the field of operations research. Mathematical modelling problems are grouped into two types: a black-box model and a white-box model. This study focuses on the black-box model. In the black-box model, the structure of the function and the numerical coefficients and constants in the function must match the given data set.

A frequent approach to a black box model is cybernetic optimization such as genetic algorithm and neural network, which usually makes no assumptions about the incoming data. Steps to building a good mathematical model include primary data processing, training, and tuning, as well as model evaluation.

In predicting the transport property of a refrigerant, existing models are analyzed based on their performance to calculate the viscosity of refrigerants. This study is to develop two types of predictive models: the ECS model using symbolic regression and the EES model using weighted least squares regression.

3.2 Extended corresponding states

Symbolic regression is one of the genetic programming methods to find the best solution to the equation using a structural method by the process of natural selection. A genetic algorithm is an optimization method proposed by Holland in his book [18]. Moreover, the genetic algorithm is well known for the best optimization than other similar methods, which use random datasets [19]. *Figure 1* shows the approach used in symbolic regression. The concept of the approach used refers to the natural evolutionary process as famously called Darwin's evolutionary theory.

The viscosity of a refrigerant has contribution factors mainly divided into three terms: dilute gas term, initial dependent term, and the residual term [9]. Viscosity value can be estimated by adding up all the contributing parameters. The viscosity values can be obtained from the ECS model by calculating the three terms first. Equation 1 shows its mathematical correlation, which has a function of temperature T and density ρ and consists of four terms.

$$\eta(\rho,T) = \eta_0(T) + \eta_1(T)\rho + \Delta\eta(\rho,T) + \Delta\eta_c(\rho,T) \quad (1)$$

The temperature has units in kelvin, whereas the density has units in kg/m^3. The first three terms are dilute gas, initial dependence, and residue. While the last term is a parameter that contributes to viscosity when the state of a fluid approaches a critical state. The first and second terms are obtained theoretically. Furthermore, further explanations will be discussed in upcoming sections. Since no experimental data for the fourth term exists near the critical point, this enhancement term is neglected. The third term $\Delta\eta$ can be obtained by fitting the input data using symbolic regression, which is obtained from available experimental data.

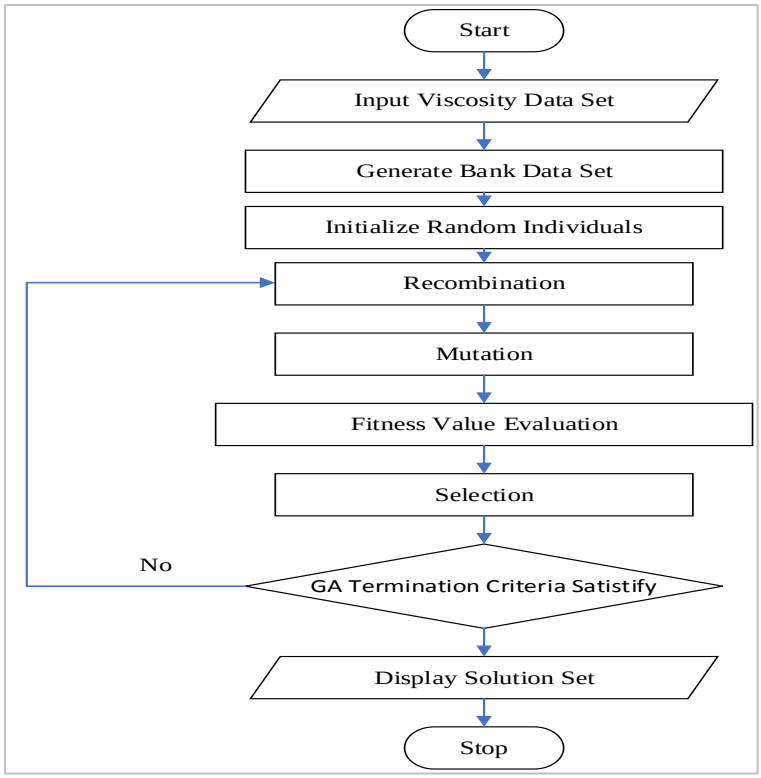

Figure 1 Genetic algorithm flowchart for modelling viscosity

The physical constants estimated with Chung's method [20] are used in theoretical calculations using the ECS model for HCFO-1233zd(E) and consist of a molecular mass of 130.49 g/mol, a critical temperature of 439.60 K, a critical pressure of 3.62 MPa, and a critical density of 480.22 kg/m^3. Experimental data are required to achieve an accurate correlation of the viscosity equation for a wide range of temperature and pressure. The input data set in the regression process comes from two sources: Meng et al. [9] and Alam [10]. The available data from Meng et al. is for the liquid phase from the temperature of 240 K up to 400 K at pressure up to 40 MPa. Other available data from Alam cover the liquid phase for a temperature of 314 K up to 434 K and pressures up to 4.07 MPa. *Figure 2* shows the distribution of data of the available data. It appears that the data is unavailable for the liquid phase at a pressure lower than 1 bar, at temperature higher than 400 K, and a pressure higher than 47 bar.

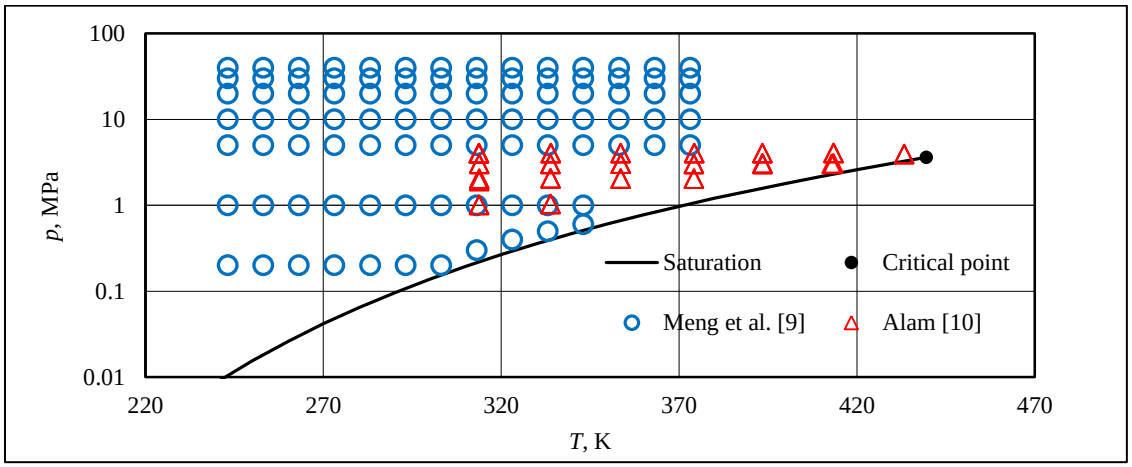

Figure 2 Experimental viscosity data distribution of HCFO-1233zd(E)

The viscosity of a dilute-gas limit is a function of temperature and depends on the parameters of molar mass, inter-molecular energy, dipole moment, and acentric factor. Equation 2 shows the relation that belongs to the contribution.

$$\eta_0(T) = \frac{0.02669\times(MT)^{\frac{1}{2}}}{\sigma^2\Omega^*}F_c \quad (2)$$

Units of parameters in the equation are μPa·s for the dilution gas limit (η_0), g/mol for the molar mass, and nm for Lennard-Jones collision diameter (σ), and the non-smooth sphere molecular effect correction factor (F_c) is unitless.

The Lennard-Jones collision integral proposed by Neufeld et al. [21] contributes to the calculation of refrigerant viscosity. This collision-integral term correlates as given in Equation 3. It has a relation to the ratio of the Boltzmann constant (k_B) and the Lennard-Jones energy parameter (ε), where this ratio symbolizes $T^* = k_B/\varepsilon$.

$$\Omega^* = \frac{1.16145}{(T^*)^{0.14874}} + \frac{0.52487}{e^{0.7732(T^*)}} + \frac{2.16178}{e^{2.43787(T^*)}} - 6.435 \times 10^{-4}(T^*)^{0.14874}\sin(18.0323(T^*)^{-0.7683} - 7.27371) \quad (3)$$

The correction factor (F_c) and the residual dipole moment (μ_r) are required to calculate the calculation of dilute-gas limit viscosity (η_0). Equations 4 and 5 are two correlations used to calculate F_c and μ_r, respectively.

$$F_c = 1 - 0.2756\omega + 0.059035\mu_r^4 + \kappa \quad (4)$$

$$\mu_r = 131.3\mu/(V_cT_C)^{1/2} \quad (5)$$

The correction factor F_c depends on an acentric factor (ω), dipole moment (μ), critical volume and temperature (V_cT_c), and the effect of hydrogen bonding of the associated substances (κ). In this study, the correction factor of the bonding effect (κ) is neglected. For interest calculation, numerical values for all the parameters included in the calculation of this study for the viscosity of dilute-gas limit are summarized in *Table 1*.

Table 1 Numerical coefficients for Equations 4 and 5

Parameter	Source	Value	Unit
Collision diameter, σ	Ref [21]	0.5240	Nm
Lennard-Joule Potential, ε/k_B	Ref [4]	349.1	K
Acentric factor, ω	Ref [4]	0.3025	-
Dipole moment, μ	Ref [22]	1.440	Debye
Hydrogen bonding correction factor, *k*	Ref [4]	0	-

The initial dependent term (η_1) in the viscosity equation is determined by conducting sequential calculation with correlation as given in Equation 6 to 8 [19, 20]. The first calculation is determining the reduced second virial coefficients (B_η^*) of the initial dependent term and then return the second virial of the viscosity (B_η). Numerical coefficients (b_i) of the reduced second virial coefficients (B_η^*) from Vogel et al. [23]were used in this study.

Numerical values of these coefficients b_0 to b_8 are -19.572881, 219.73999, -1015.3226, 2471.0125, -3375.1717, 2491.6597, -787.26086, 14.085455, and -0.34664158, respectively. The last calculation is used to Equation 8 to get the initial dependence η_1.

$$B_\eta^*(T^*) = \sum_{i=0}^{6} b_i(T^*)^{-0.25i} + b_7(T^*)^{-2.5} + b_8(T^*)^{-5.5} \quad (6)$$

$$B_\eta(T) = B_\eta^*(T^*)N_A\sigma^3 \quad (7)$$

$$\eta_1(T) = \frac{B_\eta(T)\eta_0(T)}{M_w} \quad (8)$$

A symbolic regression, which explores the space of mathematical expression to get the best model for an input data set, is used to obtain the function $F(\rho_r, T_r)$ in the residual term. The method to achieve a high-quality solution in genetic programming that works based on this type of regression requires the completion of three subs of the task that are interconnected with each other together to get the best results. The selection of the appropriate subset of variables, finding the best structural form of a model containing the variables, and a decision on desirable parameter values of the model based on the fitness of an optimization problem are three subtasks involved in the symbolic regression. In addition, the results obtained iteratively in the subtasks depend on other subtasks and the previous results to produce the desired solution. This process will improve the overall quality of the subtask results to improve the overall ability of the algorithm to get the best solution. The property data used in the development of the equation for the residual part are density ρ, temperature T, and the residual term $\Delta\eta$ calculated by subtracting the dilute gas η_0 and temperature dependence term η_1 from experimental viscosity, η.

The function in the residual term is optimized using a nonlinear regression analysis of a given dataset. The hard-sphere model of Assael et al. [24] is applied when optimizing the residual term is shown in Equation 9.

$$F(\rho_r, T_r) = \frac{\Delta\eta}{\rho_r^{\frac{2}{3}} T_r^{\frac{1}{2}}} \quad (9)$$

Initially, the program randomizes the seed using Mersenne Twister as a random number generator. Additionally, the program sets a population size based on the size set and analyses the solution using the current scope. Moreover, the evaluated solutions are stored in a variable called "Evaluated Solutions". Once the preinitiation process is ready, the genetic algorithm of the main loop can be executed. Genetic operations such as recombine, mutation, selection, probability analysis, and iteration to obtain the best solution undergo. Finally, after the symbolic regression analysis was just run, the mathematical form or a form of a tree diagram will be resulted out. *Figure 3* shows a result of the symbolic regression generated using HeuristicLab in tree diagram form. In this case, $F(\rho_r,T_r)$ as an objective function was entirely solved using the symbolic regression.

The terms $\eta_0(T)$ and $\eta_1(T)$ are obtained from Equations 2–8 based on the data points from the experimental data. The residual term can be calculated and is the result of reducing the viscosity from the experimental data by subtracting $\eta_0(T)$ and $\eta_1(T)\rho$ on a case of neglecting the critical point. A mathematical formula for calculating the residual term is obtained with functional form as given in Equation 10. As indicated in the equation, it has a function of reduced temperature T_r and reduced density ρ_r and as many as 13 coefficients must be determined in this modelling. Both reduced parameters are defined by dividing their critical parameters to make a non-dimensional number i.e., $T_r=T/T_c$ and $\rho_r = \rho/\rho_c$. This non-linear relationship causes the determination of the coefficients to be difficult. Numerical coefficients c_0 to c_{12} because of this study are listed in *Table 2*.

$$\Delta\eta(\rho_r, T_r) = \rho_r^{\frac{2}{3}} T_r^{\frac{1}{2}} \left(\left(\frac{\rho_r{}^2 c_0 c_1 c_2}{T_r \rho_r c_3 (c_4 T_r + c_5 \rho_r + c_6)(c_7 T_r + c_8) c_9} + c_{10} \right) c_{11} + c_{12} \right) \quad (10)$$

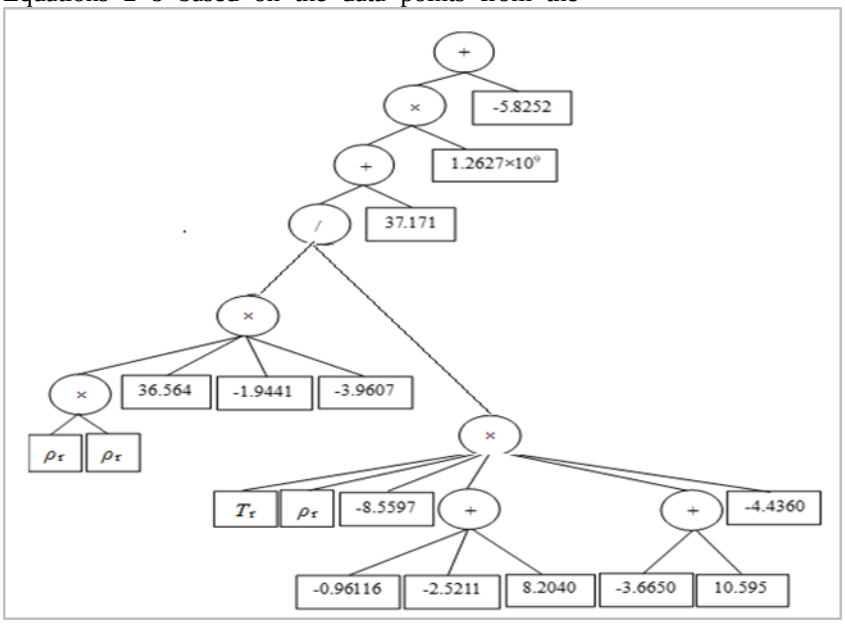

Figure 3 Tree diagram generated using HeuristicLab

Table 2 Numerical coefficients for calculating $\Delta\eta$

Parameter	Value
c_0	36.564
c_1	-194.41
c_2	-39.607
c_3	-855.97
c_4	0.96116
c_5	-2.5211
c_6	8.2040
c_7	-3.6650

Parameter	Value
c_8	10.595
c_9	-0.4436
c_{10}	37.171
c_{11}	1.2627
c_{12}	-58.252

3.3Excess entropy scaling

In this section, to prove whether there is a relationship between viscosity and entropy, a linear regression is conducted. When fitting the experimental data, a direct relationship between $\ln(\eta^*)$ and s^* is observed. The function is determined by Equation 11.

$$\ln(\eta^*) = \beta_0 + \beta_1 s^* + \varepsilon_i \quad (11)$$

The coefficients β need to be determined beforehand. To solve the equation, linear equation systems are presented in matrix notation shown in Equation 12.

$$\begin{bmatrix} \ln(\eta^*)_1 \\ \ln(\eta^*)_2 \\ \vdots \\ \ln(\eta^*)_n \end{bmatrix} = \begin{bmatrix} 1 & {s^*}_1 \\ 1 & {s^*}_2 \\ \vdots & \vdots \\ 1 & {s^*}_n \end{bmatrix} \begin{bmatrix} \beta_0 \\ \beta_1 \end{bmatrix} + \begin{bmatrix} \varepsilon_1 \\ \varepsilon_2 \\ \vdots \\ \varepsilon_n \end{bmatrix} \quad (12)$$

where matrix Y consists of $\ln(\eta^*)$ experimental values, matrix X consists of s^* experimental values, matrix B consists of coefficients β, and matrix E consists of error ε values. The solution of the equation is presented by Equation 13.

$$Y = XB + E \quad (13)$$

In case of introducing weighting factors for each data point is w_i, so that sum of weighted least squares (WLS) can be written in Equation 14.

$$WLS = \sum_{i=1}^{n} w_i \varepsilon_i^2 \quad (14)$$

The WLS is minimized in the regression process to value of matrix element in matrix B by setting each differentiation of WLS respective to each coefficient β equal zero. Based on this last setting, relation of matrix B consisting of coefficients β can be written in Equation 15.

$$B = (X^T W X)^{-1} X^T W Y \quad (15)$$

where Y is $\ln(\eta^*)$, X is s^* and β is the coefficient and matrix of W is given in Equation 16.

$$W = \begin{bmatrix} w_1 & 0 & \cdots & 0 \\ 0 & w_2 & \cdots & 0 \\ \vdots & \vdots & \ddots & \vdots \\ 0 & 0 & \cdots & w_n \end{bmatrix} \quad (16)$$

Matrix $X^T W X$ is evaluated with a relation as shown in Equation 17.

$$X^T W X = \begin{bmatrix} n\sum_{i=1}^{n} w_i & n s_i^* \sum_{i=1}^{n} w_i \\ n s_i^* \sum_{i=1}^{n} w_i & \sum_{i=1}^{n} w_i {s_i^*}^2 \end{bmatrix} \quad (17)$$

The value of s^* is estimated with using experimental data of refrigerant HCFO-1233zd(E) [9, 10]. The inverse of matrix $X^T W X$ is calculated using Equation 18.

$$(X^T W X)^{-1} = \frac{1}{n\left(\sum_{i=1}^{n} w_i s_i^* - w_i s_i^*\right)^2} \begin{bmatrix} \sum_{i=1}^{n} w_i {s_i^*}^2 & -n s_i^* \sum_{i=1}^{n} w_i \\ -n s_i^* \sum_{i=1}^{n} w_i & n \sum_{i=1}^{n} w_i \end{bmatrix} \quad (18)$$

Furthermore, the product of $X^T Y$ is evaluated using Equation 19.

$$X^T W Y = \begin{bmatrix} n \ln(\eta^*) \sum_{i=1}^{n} w_i \\ \sum_{i=1}^{n} w_i s_i^* \ln(\eta^*) \end{bmatrix} \quad (19)$$

Finally, the solution obtained after evaluating is shown in Equation 20.

$$B = \begin{bmatrix} \sum_{i=1}^{n} w_i \ln(\eta^*) - \hat{\beta}_1 \sum_{i=1}^{n} w_i s_i^* \\ \frac{\sum_{i=1}^{n} w_i (s_i^* - \overline{s_i^*})\left(\ln(\eta^*) - \ln(\overline{\eta^*})\right)}{\sum_{i=1}^{n} w_i \left(\sum_{i=1}^{n} s_i^* - \overline{s_i^*}\right)^2} \end{bmatrix}$$

$$= \begin{bmatrix} \hat{\beta}_0 \\ \hat{\beta}_1 \end{bmatrix} = \begin{bmatrix} 46.975 \\ -0.9586 \end{bmatrix} \quad (20)$$

Alternatively, a simpler way to calculate viscosity using the EES method is presented. In the classical EES method, the linear equation that is evaluated using Equation 21.

$$\ln(\eta^*) = a + b s^* \quad (21)$$

To solve the equation above, the value of entropy is needed. Like the Helmholtz equation, the entropy can be expressed as a function of density and temperature and its value can be calculated using Equation 22.

$$s^{res}(\rho, T) = s(\rho, T) - s^{id}(\rho, T) \quad (22)$$

Regarding EES method, the dimensionless viscosity can be calculated using Equation 23.

$$\eta^* = \frac{\eta}{\rho^{2/3}\sqrt{\frac{M k_B T}{N_A}}} \quad (23)$$

The reduced residual entropy can be obtained using Equation 24.

$$s^* = \frac{s^{res}(\rho,T)}{k_b M} \quad (24)$$

The result of the regression equation, which is representing the diagram as shown in *Figure 4*, can be written in Equation 25. This relation is a result accomplished of the regression under the EES.

$$\eta(\rho,T) = e^{(46.975-0.9586s^*)}\rho^{2/3}\sqrt{\frac{Mk_bT}{N_A}} \quad (25)$$

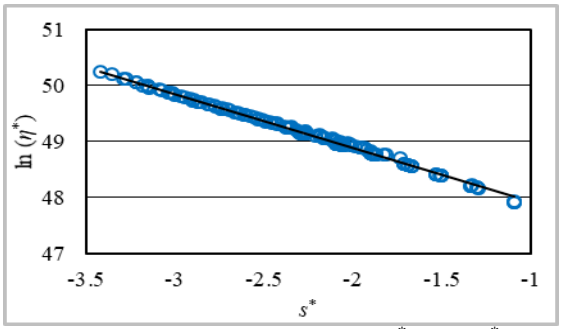

Figure 4 Correlation between ln(η^*) and s^* in the liquid phase

3.4Computer program validation

Several data points calculated used the procedures and models resulted of this study to test the equation of the modelling results. *Table 3* presents an example of the results obtained from these calculations. By inputting the data of density and temperature, the viscosity value predictions from the ECS and EES models can be calculated as a result presented in the table. These data can be used to validate models that have been included in the calculation formula either in the worksheet or in the program code. If the same result is obtained, it means that the transfer of the model to the software has been correct.

Table 3 The viscosity value from this study models

***T*, K**	**ρ, kg/m^3**	**η, µPa·s**	
		ECS	**EES**
243.14	1395.7	557.57	572.12
303.15	1250.7	269.94	270.87
353.14	1163.9	191.94	191.23
412.90	897.39	82.968	89.597

4.Results

4.1 Comparison of models

To assess which viscosity model is preferable for application, the models of ECS and EES are compared. *Table 4* shows the statistical analysis of deviation for the calculated value from the experimental data in tabular form. The analysis measure considered are average absolute deviation (AAD), standard deviation of the deviations (STD), maximum absolute deviation (MAX), and average of the deviations (BIAS).

Table 4 Statistical analysis of this study models

Parameter		**Data Source**		
		Meng et al. [9]	**Alam** [10]	**otal**
MAX	ECS	7.72	6.23	7.72
%	EES	6.28	10.6	10.6
AAD	ECS	1.61	1.56	1.59
%	EES	1.82	2.16	1.96
STD	ECS	1.96	2.09	2.05
%	EES	2.13	2.18	2.72
BIAS	ECS	0.520	1.44	1.07
%	EES	1.25	-2.16	-0.109
Point		92	61	153

The deviation of calculated viscosity value with respect to experimental data of Meng et al. [9] and Alam [10] using the ECS model has a deviation ranging from -2.33% to 7.72% at temperatures from 243 K to 433 K as shown in *Figure 5*. Moreover, the deviation of calculated viscosity value with respect to experimental data of Meng et al. [9] and Alam [10] using the ECS model has a deviation ranging from -10.6% to 6.28% at temperatures ranging from 243 K to 433 K. The experimental data of Alam can be represented by the ECS model within a deviation of 10%, which is better than the previous model used. However, the data of Meng et al. is represented by the ECS model as slightly inferior in higher temperatures than their correlation.

In summary, the deviation of the calculated value using the ECS model has an AAD of 1.59% and the calculated value using the EES model has an AAD of 1.96%, hence the ECS model is more accurate in calculating the viscosity value of HCFO-1233zd(E).

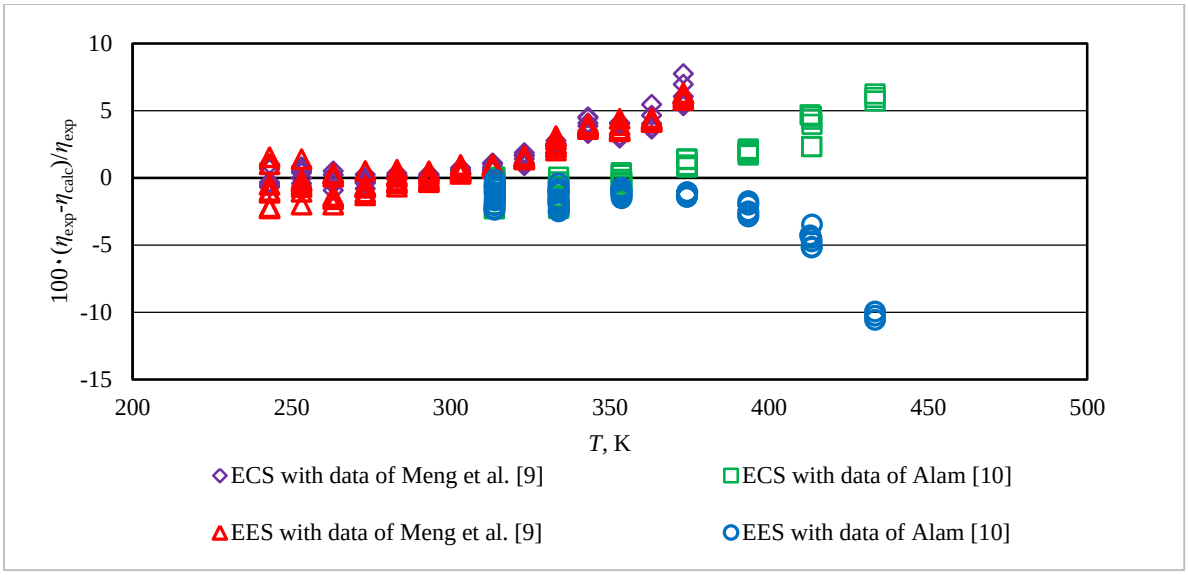

Figure 5 Deviation of calculated value of ECS and EES models to the experimental data

4.2Data visualization of best model

Using the developed model of the ECS model, the viscosity as a transport property of refrigerant HCFO-1233zd(E) can be visualized. By visualizing the data, it is easy to identify correlations between thermodynamic and transport properties.

Moreover, the program used to create patterns and graphs in this work is Python [25]. In refrigerants, the most common way to understand the correlation of transport properties with thermodynamic properties is by visualizing the *p-T-η* graph. Furthermore, the correlation of viscosity with respect to experimental data of temperature and pressure used on the modelling is visualized in *Figures 6 to Figure 8.*

Effect tendency of increasing pressure to viscosity can be observed from *Figure 6.* On the increasing of temperature causes decreasing viscosity of the liquid phase as shown in *Figure 7*. Effect tendency of pressure and temperature are simultaneously represented in *Figure 8.*

In this work, the ability to extrapolate viscosity for temperatures from 200 up to 500 K and pressures from 0.1 MPa up to 50 MPa is visualized. Based on the data visualization, the saturated viscosity lines of a refrigerant at the liquid phase can be drawn and the points at which the viscosity is in the liquid phase or gaseous phase by its density value can be determined.

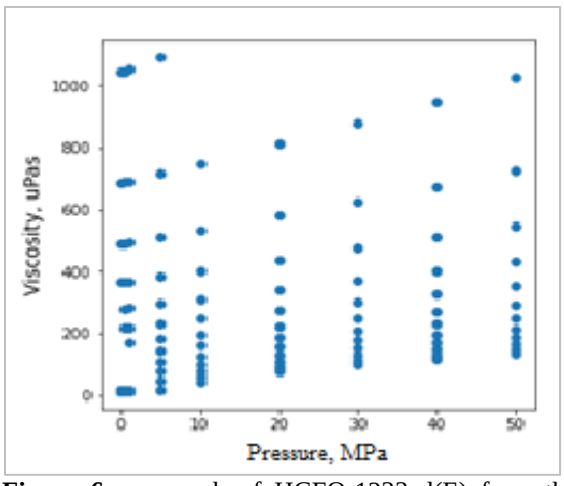

Figure 6 *η-p* graph of HCFO-1233zd(E) from the new ECS model

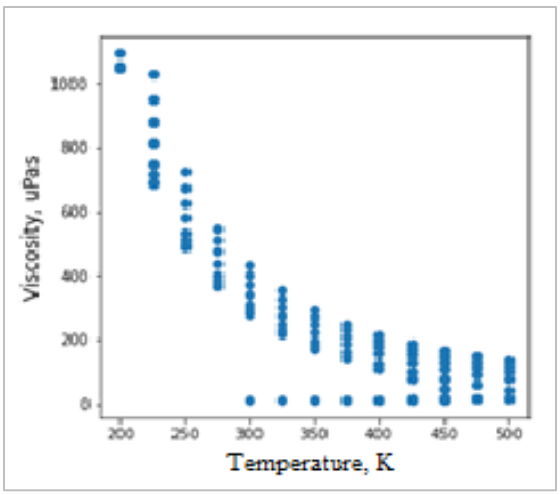

Figure 7 *η-T* graph of HCFO-1233zd(E) from the new ECS model

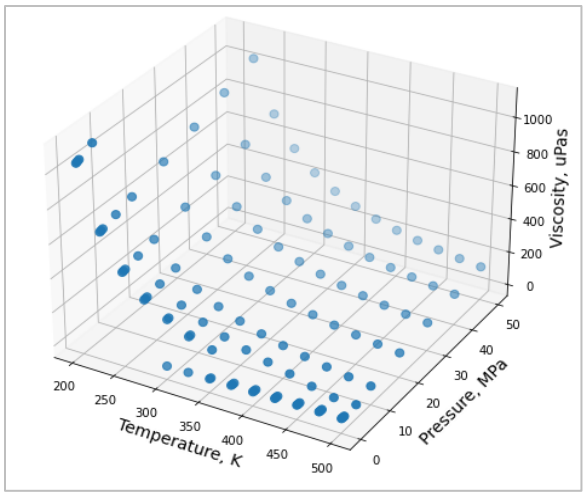

Figure 8 *p-T-η* graph of HCFO-1233zd(E) from the new ECS model

The ability to extrapolate the viscosity using the new ECS model is presented in *Figure 9*. Reasonable extrapolation was conducted for temperatures from 200 K up to 450 K and pressures from 0.1 up to 50 MPa. It can be observed that the extrapolated curve still shows a suitable pattern in this range. At the constant pressure line above the pressure of 10 MPa, the viscosity starts at a temperature of 225 K. These conditions indicate a liquid phase. On the other hand, extrapolation of viscosity in the gas phase is not possible. In theory, the gas-phase viscosity should be below the saturated vapor line.

Figure 10 shows the extrapolation of constant temperature lines is ranged for temperatures from 200 K up to 450 K and pressures from 0.1 MPa up to 50 MPa. The isothermal graph shows a straight curve that correlates the relationship between viscosity and pressure. If the pressure increases and the temperature decreases, then the viscosity increases. The viscosity values at 200 K indicate that it stops at the pressure of 5 MPa, and the constant temperature line continues until 50 MPa with temperatures above 225 K. The vertical lines on each isobaric line indicate saturation conditions.

It is challenging to obtain a viscosity model that can be applied to the fluid phase, not only in the liquid but also in the gas phase. A simpler model having a theoretical basis is needed to gain confidence in its reliability in presenting viscosity in a state where the test is difficult to measure. Due to the limited data available in this model, the two viscosity models discussed in this article are applicable only in the liquid phase.

More research attention to obtaining environmentally friendly refrigerants has led to greater attention to thermodynamic properties. Viscosity, which affects the pressure loss and heat transfer process, has received less attention. This situation causes the experimental data to be very lacking, especially in the gas phase. Furthermore, viscosity data of HFO refrigerant included in a new type of refrigerant group is still very limited compared to its predecessor generation refrigerant.

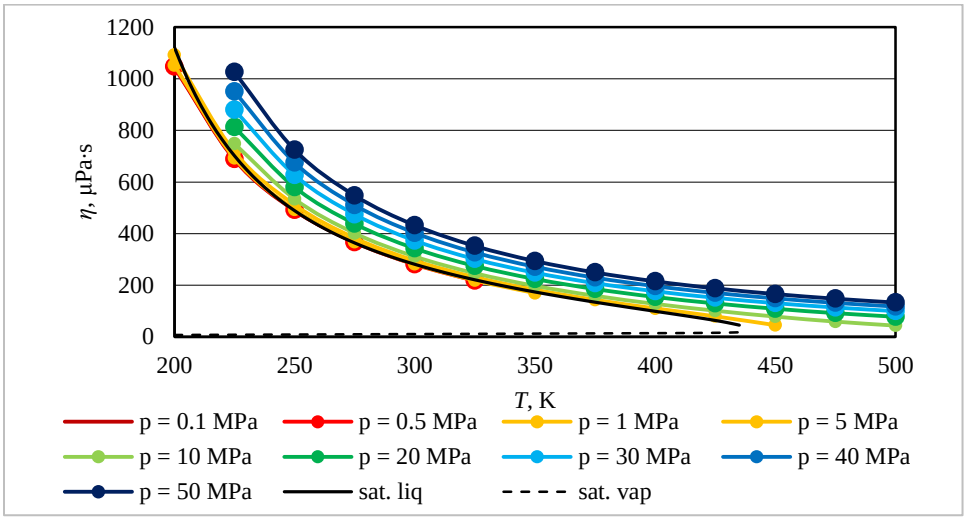

Figure 9 Isobaric line of viscosity of HCFO-1233zd(E)

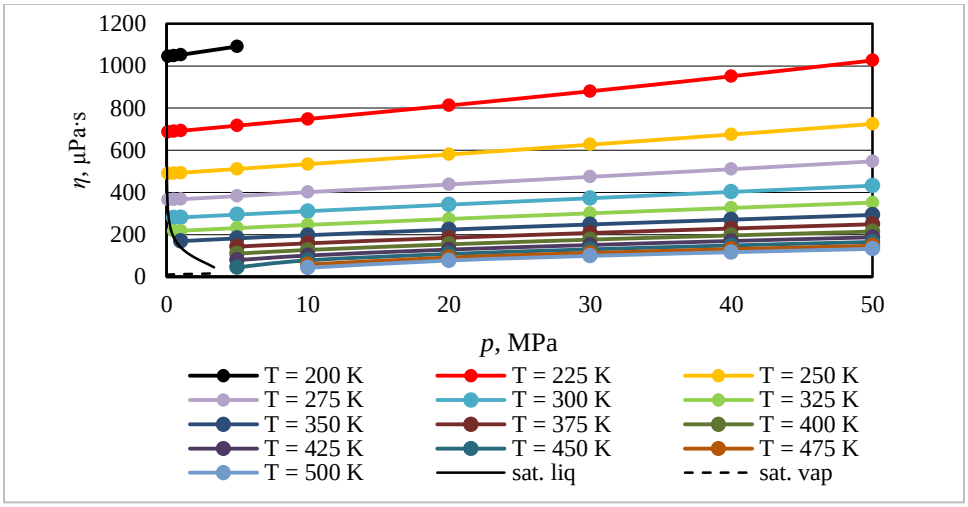

Figure 10 Isothermal graph of viscosity of HCFO-1233zd(E)

5.Discussion

This section summarizes the findings, interpretations, and recommendations, along with the future direction of the study. Limited data cause difficulty in obtaining a model that can be applied over a wide range of pressures and temperatures. The available data for HCFO-1233zd(E) is still limited, and filtering to obtain an accurate one difficultly. Differences in the accuracy of data from one source to another can cause difficulties in fitting the model to the data. In this study, the two data sources used with different temperature ranges allow the model to have a wider validation range, but this difference in accuracy makes it difficult to obtain low deviations at higher temperatures for the data of Alam [10]. Data from Meng et al. [9] has a higher accuracy, both expressed by the EES model and with the ECS giving low deviation.

Impact of parameters such as physical properties and thermodynamical properties of refrigerants are being used to conduct mathematical modelling for viscosity prediction. These two approaches have resulted in the flow of viscosity modeling based on entropy and corresponding state. These two streams have been applied to the viscosity modeling carried out in this study. Besides these two approaches, an empirical approach can also be applied to obtain mathematical models of both thermodynamic and transport properties. To get a valid model in a wide range, this empirical approach needs the support of a lot of input data. Viscosity is directly proportional to pressure hence, as the pressure increase, the viscosity tends to increase. However, the increasing viscosity at lower pressure disconnect at saturation points. Similarly, viscosity is also directly proportional to temperature. The viscosity decreases as temperature decrease due to the decreasing molecular forces that are happening microscopically. To prove this statement, it is well known that when heating liquid, it gets less viscous over time.

The predicted viscosity also differs with different modeling techniques used. Due to the lack of experimental data for this specific refrigerant, the model proposed in this paper can be improved by using more thermal properties of refrigerants, decreasing the mean absolute error of the model as minimum as possible and the complexity of the model used. To increase the value of viscosity prediction accuracy, the recommended model to be used is the artificial neural network model which has been implemented in various fields in the world. Furthermore, increasing the data collected for input data from input data sets such as temperature, density and pressure will drastically improve the accuracy of the model. The accuracy of each of these data plays a role in the accuracy of the developed model.

A complete list of abbreviations is shown in *Appendix I.*

6.Conclusion

This work developed and compared the two viscosity models. The ECS and EES models were selected as a predictive method for low GWP HCFO-1233zd(E). The developed ECS model has an AAD of 1.59%, MAX of 7.72%, STD of 2.05%, and BIAS of 1.07%, while the developed EES model has an AAD of 1.96%, MAX of 10.6%, STD of 2.72%, and BIAS of -0.109%. Based on the comparative analysis, the ECS model is more suitable for the application. These

differences are caused by considerations of Lennard-Joule's parameters and collision integrals. The newly developed ECS model has better accuracy than the EES model in predicting viscosity value. Visualization correlation based on the ECS model for pressure, temperature, and viscosity of HCFO-1233zd(E) in the liquid phase and experimental data plot was plotted to confirm consistency relations. A proper extrapolation behavior of the ECS model to calculate viscosity in the liquid phase for temperatures from 200 K up to 500 K and pressures from 0.1 MPa up to 50 MPa was confirmed.

Acknowledgment
None.

Conflicts of interest
The authors have no conflicts of interest to declare.

Author's contribution statement
Donny Agvie Putratama: Conceptualization, investigation, data curation, writing original draft, writing, and editing. **I Made Astina:** Study conception, design, supervision, manuscript review and revision, and final decision.

References
[1] Solomon S, Qin D, Manning M, Chen Z, Marquis M, Averyt KB, et al. Contribution of working group I to the fourth assessment report of the intergovernmental panel on climate change. Cambridge, 2007.
[2] Ziviani D, Dickes R, Quoilin S, Lemort V, De PM, Van DBM. Organic rankine cycle modelling and the ORCmKit library: analysis of R1234ze (Z) as drop-in replacement of R245fa for low-grade waste heat recovery. In the 29th international conference on efficiency, cost, optimization, simulation and environmental impact of energy systems 2016 (pp. 1-13).
[3] Tsvetkov OB, Laptev YA, Sharkov AV, Mitropov VV, Fedorov AV. Alternative refrigerants with low global warming potential for refrigeration and air-conditioning industries. In IOP conference series: materials science and engineering 2020 (pp. 1-4). IOP Publishing.
[4] https://www.ashrae.org/technical-resources/standards-and-guidelines/standards-addenda/ansi-ashrae-standard-34-2013-designation-and-safety-classification-of-refrigerants. Accessed 26 July 2022.
[5] Mondejar ME, Mclinden MO, Lemmon EW. Thermodynamic properties of trans-1-chloro-3, 3, 3-trifluoropropene (R1233zd (E)): vapor pressure,(p, ρ, T) behavior, and speed of sound measurements, and equation of state. Journal of Chemical & Engineering Data. 2015; 60(8):2477-89.
[6] Orkin VL, Martynova LE, Kurylo MJ. Photochemical properties of trans-1-chloro-3, 3, 3-trifluoropropene (trans-CHCL=CHCF3): OH reaction rate constant, UV and IR absorption spectra, global warming potential, and ozone depletion potential. The Journal of Physical Chemistry A. 2014; 118(28):5263-71.
[7] Hulse RJ, Basu RS, Singh RR, Thomas RH. Physical properties of HCFO-1233zd (E). Journal of Chemical & Engineering Data. 2012; 57(12):3581-6.
[8] Yin J, Ke J, Zhao G, Ma S. Experimental vapor pressures and gaseous pvT properties of trans-1-Chloro-3, 3, 3-trifluoropropene (R1233zd (E)). International Journal of Refrigeration. 2021; 121:253-7.
[9] Meng X, Wen C, Wu J. Measurement and correlation of the liquid viscosity of trans-1-chloro-3, 3, 3-trifluoropropene (R1233zd (E)). The Journal of Chemical Thermodynamics. 2018; 123:140-5.
[10] Alam MJ. Measurements and prediction of transport properties of low GWP refrigerants. Saga University, Saga. 2018.
[11] Cui J, Yan S, Bi S, Wu J. Saturated liquid dynamic viscosity and surface tension of trans-1-chloro-3, 3, 3-trifluoropropene and dodecafluoro-2-methylpentan-3-one. Journal of Chemical & Engineering Data. 2018; 63(3):751-6.
[12] Zhao G, Yuan Z, Zhang X, Yin J, Ma S. Saturated liquid kinematic viscosity, surface tension and thermal diffusivity of two low-GWP refrigerants 3, 3, 3-trifluoropropene (R1243zf) and trans-1-chloro-3, 3, 3-trifluoro-1-propene (R1233zd (E)) by light scattering method. International Journal of Refrigeration. 2021; 127:194-202.
[13] Budiarso G, Astina IM, Development of Helmholtz equation of state for thermodynamic properties of R-1233zd(E). International Journal of Scientific Research in Science and Technology. 2022; 9(3):765–76.
[14] Akasaka R, Lemmon EW. An international standard formulation for trans-1-Chloro-3, 3, 3-trifluoroprop-1-ene [R1233zd (E)] covering temperatures from the triple-point temperature to 450 K and pressures up to 100 MPa. Journal of Physical and Chemical Reference Data. 2022; 51(2).
[15] Teraishi R, Kayukawa Y, Akasaka R, Saito K. Universal parameters of the extended corresponding states (ECS) model for hydrofluoroolefin refrigerants. International Journal of Refrigeration. 2021; 131:33-40.
[16] Fouad WA, Vega LF. Transport properties of HFC and HFO based refrigerants using an excess entropy scaling approach. The Journal of Supercritical Fluids. 2018; 131:106-16.
[17] Li X, Kang K, Gu Y, Wang X. Viscosity prediction of pure refrigerants applying the residual entropy scaling theory coupled with a "Generalized Chart" parametrization method for the statistical associating fluid theory. Journal of Molecular Liquids. 2022.
[18] Holland JH. Adaptation in natural and artificial systems: an introductory analysis with applications to biology, control, and artificial intelligence. MIT Press; 1992.
[19] Algdamsi H, Alkouh A, Agnia A, Amtereg A, Alusta G. Integration of self organizing map with MLFF

neural network to predict oil formation volume factor: north africa crude oil examples. In international petroleum technology conference 2020. OnePetro.
[20] Chung TH, Ajlan M, Lee LL, Starling KE. Generalized multiparameter correlation for nonpolar and polar fluid transport properties. Industrial & Engineering Chemistry Research. 1988; 27(4):671-9.
[21] Neufeld PD, Janzen AR, Aziz R. Empirical equations to calculate 16 of the transport collision integrals Ω (l, s)* for the Lennard-Jones (12–6) potential. The Journal of Chemical Physics. 1972; 57(3):1100-2.
[22] Rainwater JC, Friend DG. Second viscosity and thermal-conductivity virial coefficients of gases: extension to low reduced temperature. Physical Review A. 1987; 36(8).
[23] Vogel E, Kuechenmeister C, Bich E, Laesecke A. Reference correlation of the viscosity of propane. Journal of Physical and Chemical Reference Data. 1998; 27(5):947-70.
[24] Assael MJ, Dymond JH, Patterson PM. Correlation and prediction of dense fluid transport coefficients. V. Aromatic hydrocarbons. International Journal of Thermophysics. 1992; 13(5):895-905.
[25] Van RG, Drake FL. Python 3 reference manual. Scotts Valley, CA: CreateSpace; 2009.

Donny Agvie Putratama obtained his B.Sc.Eng degree and graduated from Institut Teknologi Bandung. His area of research interest are primarily in the areas of Data Modelling, Data Analytics, and Data Warehousing.

Email: donny.ap1997@gmail.com

I Made Astina is an Associate Professor at the Faculty of Mechanical and Aerospace Engineering, Institut Teknologi Bandung, Indonesia. He received a B.Sc.Eng. degree from Institut Teknologi Bandung, Indonesia, M.Sc.Eng. and Ph.D. degrees from Keio University, Japan. His research interests are primarily in the areas of Modelling and Database of Fluid Properties, and Energy Utilization in Buildings and Thermal Systems.
Email: astina@itb.ac.id

Appendix I

S. No.	Abbreviation	Description
1	a	Second Virial Coefficient
2	AAD	Average Absolute Deviation
3	AI	Artificial Intelligence
4	b	Coefficient of Collision Integral Equation
5	BIAS	Average of Deviation
6	c	Coefficient of Functional Form $F(\rho_r,T_r)$
7	B_η	Second Viscosity Virial Coefficient
8	CFC	Chloro Fluoro Carbon
9	ECS	Extended Corresponding State
10	EES	Excess Entropy Scaling
11	EOS	Equation of State
12	F_c	Non-smooth Sphere Molecular Effect Correction Factor
13	GWP	Global Warming Potential
14	HCFO	Hydro Chloro Fluoro Olefin
15	HFO	Hydro Fluoro Olefin
16	HFC	Hydro Fluoro Carbon
17	k_b	Boltzmann Constant
18	M	Molar Mass
19	MAX	Maximum Absolute Deviation
20	N_A	Avogadro's Constant
21	ODP	Ozone Depletion Potential
22	P	Pressure
23	R	Pearson Correlation Coefficient
24	s	Entropy
25	STD	Standard Deviation
26	T	Temperature
27	V	Specific Volume
28	σ	Lennard-Jones Size Parameter
29	Ω	Lennard-Jones Collision Integral
30	η	Viscosity
31	σ	Lennard-Jones Collision Diameter
32	Ω	Lennard-Jones Collision Integral
33	ε	Lennard-Jones Energy Parameter
34	ω	Acentric Factor